PROGRESS IN COLOR, COLORANTS AND COATINGS

available online @ www.pccc.icrc.ac.ir

Prog. Color Colorants Coat. 9 (2016), 163-171

Ministry of Science, Research and Technology
Institute for Color Science and Technology

Photocatalytic Degradation of Textile Dyes Using Ozonation and Magnetic Nickel Ferrite Nanoparticle

N. M. Mahmoodi*

Department of Environmental Research, Institute for Color Science and Technology, P. O. Box: 16765-654, Tehran, Iran.

ARTICLE INFO

Article history:
Received: 17 Feb 2016
Final Revised: 02 Jun 2016
Accepted: 07 Jun 2016
Available online: 07 Jun 2016

Keywords:
Synthesis
Nickel ferrite nanoparticle
Photocatalytic ozonation
Dye degradation
Operational parameter

ABSTRACT

Dye photodegradation using ozone and Nickel ferrite nanoparticle (NFN) as a photocatalyst was studied. The catalyst was synthesized and characterized by FT-IR, SEM and XRD. Textile dyes including Remazol Red RB (RRRB) and Direct Green B (DGB) were degraded as model compounds. Dye degradation was investigated using UV–Vis and ion chromatography (IC) analyses. The effect of catalyst dosage, pH, salt and initial dye concentration on decolorization was studied. Carboxylic acids were detected as intermediates. It can be concluded that Nickel ferrite nanoparticle could be used as an effective catalyst for photocatalytic ozonation of dyes in colored wastewater. Prog. Color Colorants Coat. 9 (2016), 161-171© Institute for Color Science and Technology.

1. Introduction

The toxicity of some dyes to the aquatic life and damaging to the aesthetic nature of the environment are severe problems due to the discharge of colored wastewater into natural streams. Thus, development of more effective methods to treat colored wastewater is an urgent need. Several physical, chemical and biological methods are used to remove dyes from wastewater [1-9]. Ozonation is one of the effective chemical oxidation methods to degrade pollutants [10-12]. Ozonation of pollutants occurs via two routes: (1) direct molecular ozone reactions, and (2) indirect pathway leading to ozone decomposition and the generation of hydroxyl radicals (OH•). The reaction of ozone with organics produces aldehyde and carboxylic acids, both of which do not react with ozone. This is the main limitation of ozone to mineralize the organics. In addition, ozonation is a relatively slow and selective process. Therefore, radical processes have to be implemented. Reaction of radical with pollutants is fast and nonselective. In contrast to ozonation alone, photocatalytic ozonation allows for the effective formation of hydroxyl radicals [10].

Catalyst nanoparticle facilitates the decomposition of ozone and hydroxyl radical formation during the photocatalytic ozonation. It should provide fast and more effective degradation and mineralization of organics. Several catalysts have been proven to be effective in the enhancement of photocatalytic ozonation efficiency [13-25]. A literature review showed that the photocatalytic ozonation of Nickel

*Corresponding author: mahmoodi@icrc.ac.ir

ferrite nanoparticle (NFN) was not investigated.

In this paper, photocatalytic ozonation of dyes using NFN was investigated. The NFN was synthesized and characterized by FTIR, SEM and XRD. Remazol Red RB (RRRB) and Direct Green B (DGB) were used as dye models. UV–Vis and Ion chromatography (IC) analyses were employed to study dye decolorization and degradation. The effect of operational parameters on decolorization such as NFN dosage, pH, salt and initial dye concentration was studied.

2. Experimental

Remazol Red RB (RRRB) and Direct Green B (DGB) were obtained from CIBA. Other chemicals were of analytical grade and obtained from Merck and used as received.

Photocatalyst synthesis: nickel nitrate (4.85 g) and iron nitrate (26.93 g) was dissolved in distilled water and added to solution (citric acid (CA), distilled water and ethylene glycol (EG)). It was heated for 2h at 80 °C. Then temperature was raised to 90–110 °C. It accelerated esterifications between CA and EG and produced a clear and viscous brown resin. It was heated to decompose organic constituents. The powder was calcined on alumina crucible for 1 h at 600 °C.

FT-IR spectrum of catalyst nanoparticle was recorded by Perkin Elmer FT-IR spectrophotometer. The morphology of catalyst was investigated by a LEO 1455VP scanning electron microscopic model LEO 1455 VP. The synthesized nanoparticle behavior was studied by X-ray diffraction model Siemens D-5000 diffractometer with Cu Kα radiation (λ = 1.5406 A °) at room temperature.

Dye degradation was done in a batch photoreactor with a UV-C lamp (9W, Philips). The ozone was generated using an Ozonica Series generator from Ozoneab Co. The oxygen flow rate was 0.08 L/min. The ozone gas concentration was measured in the reactor inlet with an ozone analyzer (Orbisphere model 3600, Switzerland).

Experiments were performed using a 1 L solution containing specified concentration of dye with 5 mg/L of NFN nanoparticle. The solution pH was adjusted using H_2SO_4 or NaOH. Samples were withdrawn from sample point at certain time intervals and analyzed for decolorization and degradation.

Decolorization of dyes was checked by measuring the absorbance at maximum wavelength (λ_{max}) of dyes (520 nm for RRRB and 634 nm for DGB) at different time intervals by UV–Vis spectrophotometer (Perkin-Elmer Lambda 25 spectrophotometer).

Ion chromatograph (METROHM 761 Compact IC) was used to assay the appearance of carboxylic acids formed during the degradation of dyes (Solution: 1 L, Dye: 150 mg/L, NFN nanoparticle: 5 mg/L, pH: 3 at room temperature (25 °C)) using an METROSEP anion dual 2, flow 0.8 ml/min, 2 mM $NaHCO_3$/1.3 mM Na_2CO_3 as an eluent, temperature 20 °C, pressure 3.4 MPa and conductivity detector.

3. Results and discussions

3.1. Characterization of NFN nanoparticle

The FT-IR spectrum of NFN is shown in Figure 1. NFN has two peaks at 3450 cm^{-1} and 500-600 cm^{-1} which indicate O-H stretching vibration and metal-oxygen vibration, respectively [26]. The OH bending of the adsorbed molecular water on catalyst was showed at 1615 cm^{-1}.

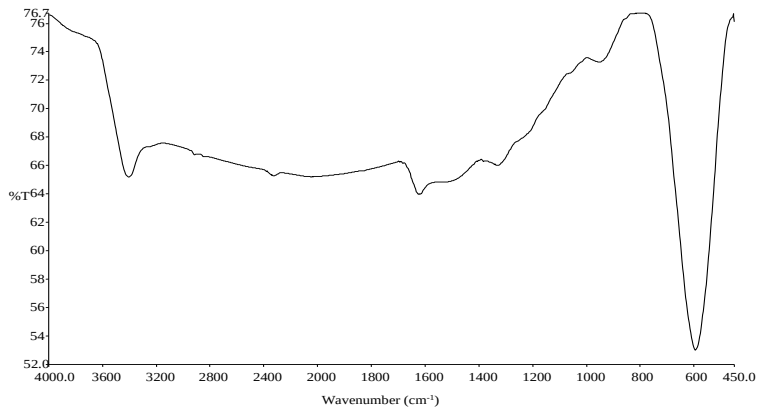

Figure 1: The FT-IR spectrum of NFN.

The SEM micrograph of the $NiFe_2O_4$ (Figure 2) shows a relatively homogeneous grain distribution, which was made up of nanosized particles (< 80 nm). Figure 3 illustrates the XRD pattern of the NFN. The results showed that spinel was formed as the most intense (311) peak and Miller indices (111), (220), (400), (422), (511) and (440) matched well with the reflections of the nickel ferrite reported in the previous published paper [27].

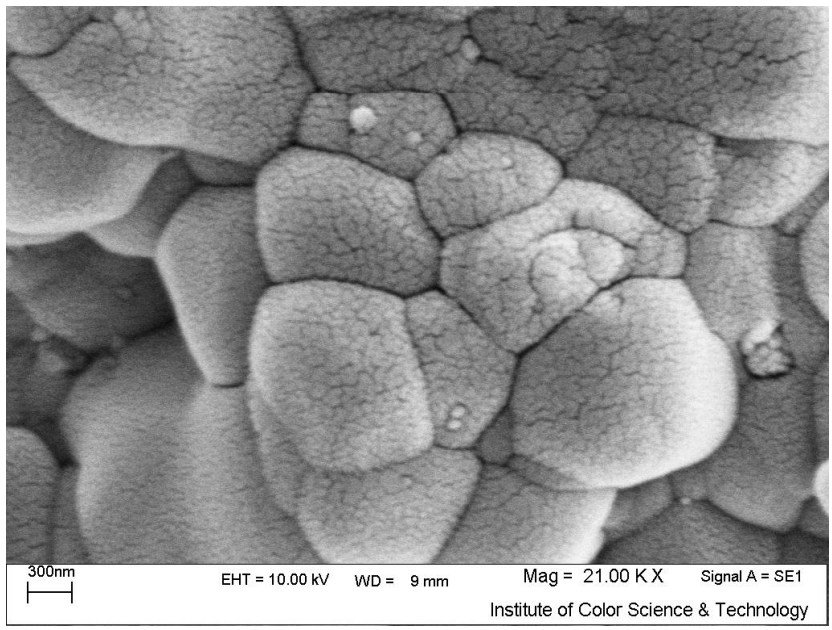

Figure 2: SEM micrograph of the synthesized nickel ferrite particles.

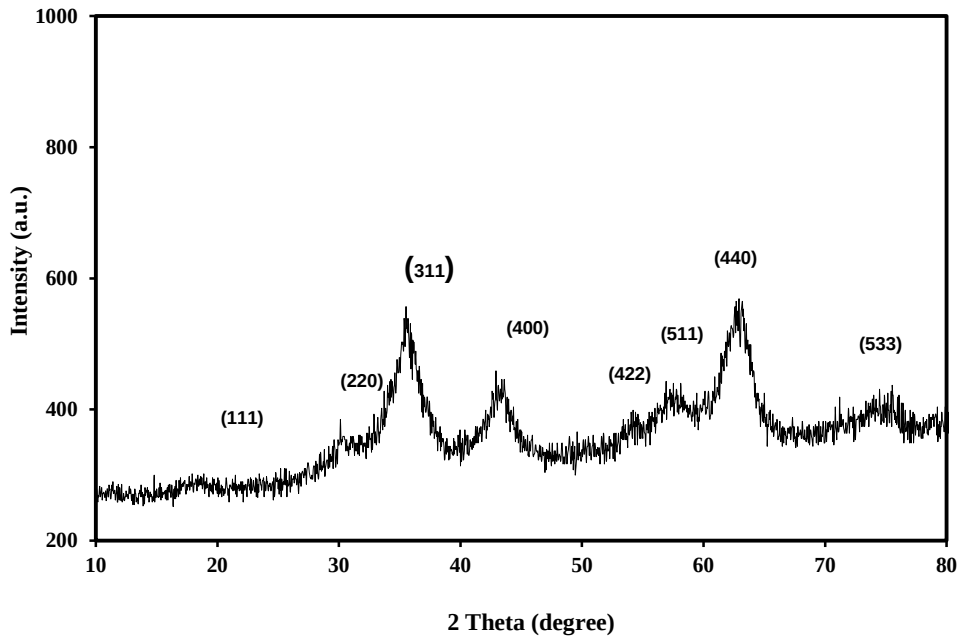

Figure 3: XRD pattern of NFN.

3.2. Degradation and mineralization of dyes

Changes of dyes absorptions within 250 nm ≤ λ ≤ 650 nm during the photocatalytic ozonation degradation using *NFN* at different time intervals of irradiation were studied. With irradiation time elapse of 20 min, the maximum absorbance in visible region of UV-Vis spectra decreased rapidly, which indicates that chromophore in both dyes are the most active sites for oxidation attack.

Further hydroxylation of aromatic intermediates leads to the cleavage of the aromatic ring resulting in the formation of oxygen-containing aliphatic compounds [28]. Formate, acetate and oxalate were detected as important aliphatic carboxylic acid intermediates during the degradation of dyes (Figure 4). The formation of aliphatic carboxylic acid intermediates initially increased with the illumination time, and then sharply dropped. Carboxylic acids can react with oxidants and generates CO2 [29].

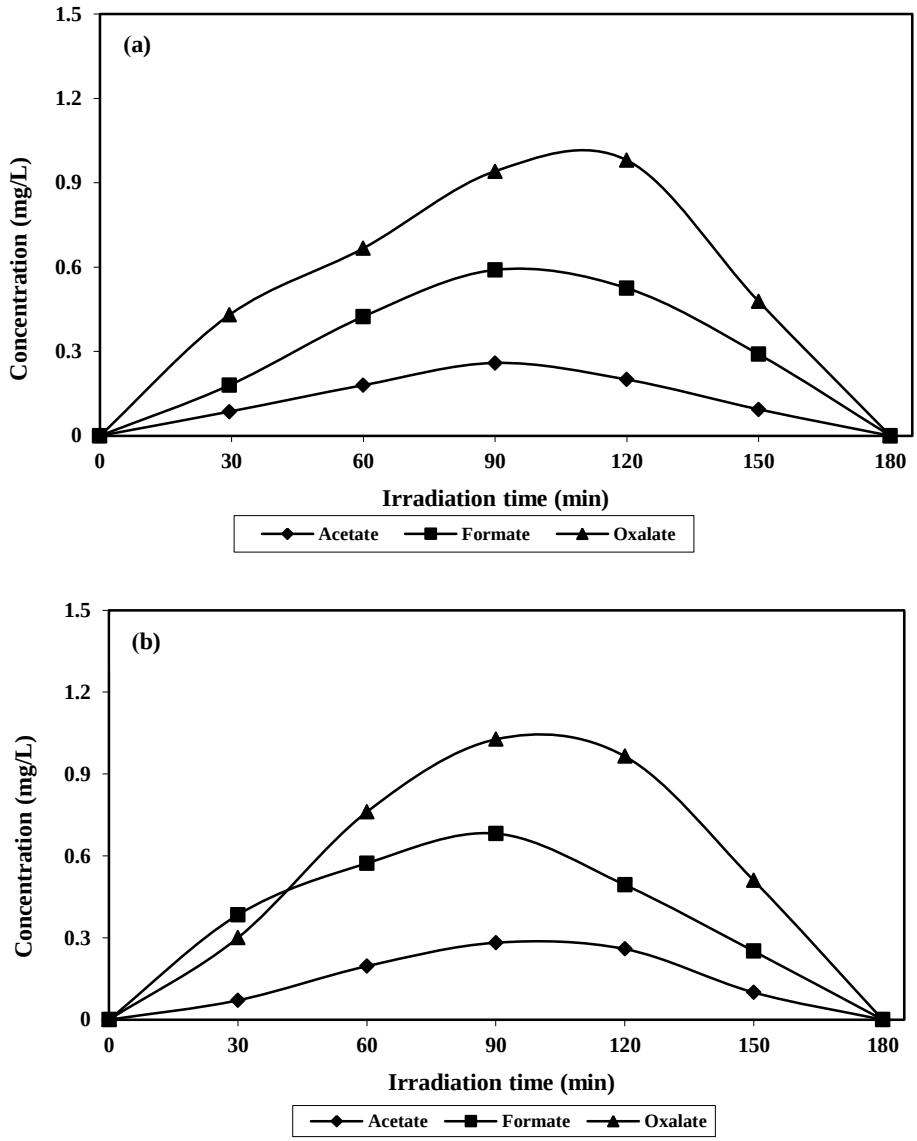

Figure 4: Formation and disappearance of aliphatic carboxylic acids during the photocatalytic ozonation of dyes (a) RRRB and (b) DGB (5 mg/L of NFN, Ozone concentration: 55 g/m^3, 1 L of dye solution (150 mg/L) and pH=3 at room temperature (25 °C)).

3.3. Effects of reaction parameters on dye degradation

The effects of reaction parameters such as NFN nanoparticle dosage, pH, anions (Cl^-, HCO_3^- and CO_3^{2-}) and dye concentration were investigated on photocatalytic ozonation of dyes.

Figure 5 shows the dye degradation as a function of illumination time when different NFN nanoparticle dosages were used. As it can be seen from Figure 5, photocatalytic ozonation with NFN nanoparticle (UV/O_3/NFN nanoparticle) has higher dye degradation efficiency than that of photoozonation (UV/O_3) due to catalytic effect of NFN nanoparticle. In addition, there is a slight increasing effect of NFN nanoparticle dosage on degradation rate of dyes, but a further increase of NFN nanoparticle dosage (up to 5 mg/L) does not lead to any improvement of dye degradation rate. This behavior is typical of photocatalytic oxidation processes that always have a critical catalyst dosage above which, due to light penetration problems, the apparent reaction rate is inhibited [10, 30].

The pH of the wastewater is one of the important parameters that determine the efficiency of ozonation since it can alter degradation pathways. Thus, comparative experiments were performed at pH range of 3-9 (Figure 6).

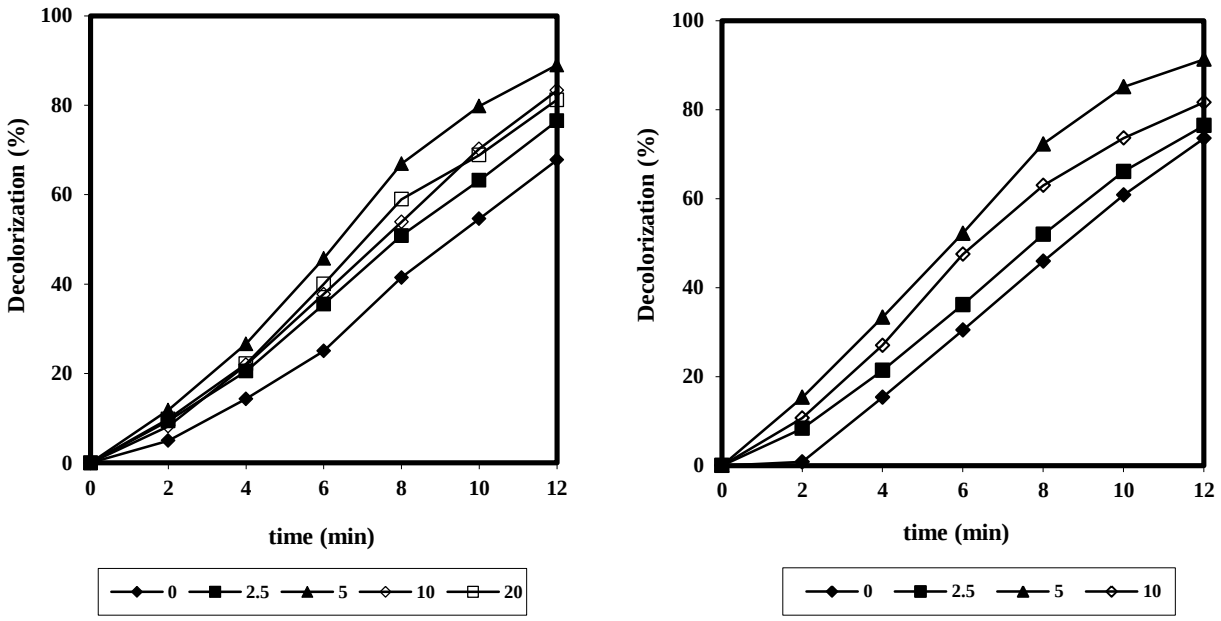

Figure 5: The effect of NFN dosage (mg/L) on the decolorization of dyes using photocatalytic ozonation (a) RRRB and (b) DGB (pH=3, Ozone concentration: 55 g/m^3, and 1 L of dye solution (150 mg/L) at room temperature (25 °C)).

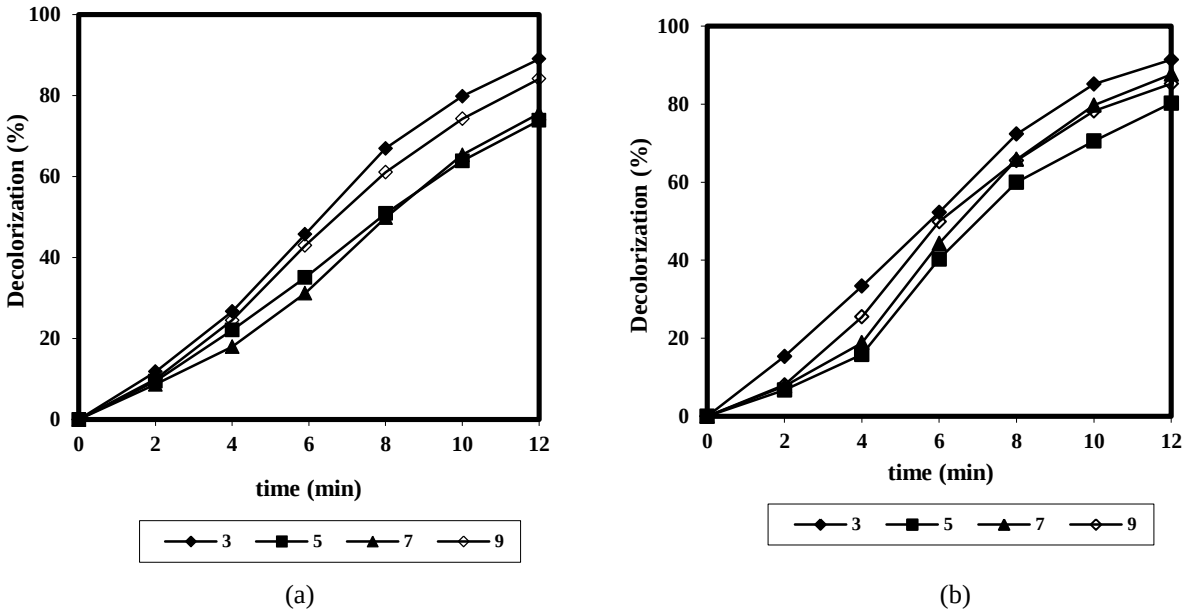

Figure 6: The effect of pH on the decolorization of dyes using photocatalytic ozonation (a) RRRB and (b) DGB (5 mg/L of NFN, Ozone concentration: 55 g/m^3, and 1 L of dye solution (150 mg/L) at room temperature (25 °C)).

Figure 6 shows that dye degradation decreases by increasing pH. Ozone decomposition in water is strongly pH-dependent and occurs faster with an increase of pH. Ozone has two mechanisms through which can degrade organic pollutants at different pH values, namely (i) direct electrophilic attack and (ii) indirect attack through the formation of hydroxyl radicals. Direct attack by molecular ozone (commonly known as ozonolysis) occurs at acidic or neutral conditions and is a selective reaction resulting in the formation of carboxylic acids as end products that cannot be oxidized further by molecular ozone. At high pH values, ozone decomposes to non-selective hydroxyl radicals. Photocatalytic ozonation allows for the effective formation of hydroxyl radicals even at low pH [10, 11]. Photocatalytic ozonation utilizes NFN nanoparticles catalysts in order to achieve controlled decomposition of ozone and hydroxyl radical formation. Therefore both direct electrophilic attack and indirect attack through the formation of hydroxyl radicals occurred at a low pH in photocatalytic ozonation.

The occurrence of inorganic anions is rather common in colored industrial wastewater. These substances may compete for the active sites on the NFN nanoparticle surface or deactivate the catalyst and, subsequently, decrease the decolorization rate of the target dyes. An important drawback resulting from the high reactivity of active species such as radicals is that they react with non-target compounds present in the background water matrix, i.e. dye auxiliaries present in the exhausted reactive dye bath. It results in higher active species demand for accomplish the desired degree of degradation, or complete inhibition of advanced oxidation rate and efficiency [31].

To study the effect of dye concentration on the rate of decolorization, the dye concentration was varied from 50 mg/L to 200 mg/L while other variables were kept constant (Figure 8). The degradation rate depends on the initial concentration of dye. As expected, the decolorization rate decreased by increasing the dye concentration.

With the increase of dye concentration, the possible reason is the interference of intermediates formed during degradation of parental dye molecules. Such suppression would be more pronounced in the presence of an elevated level of degradation intermediates formed upon an increased initial dye concentration [29].

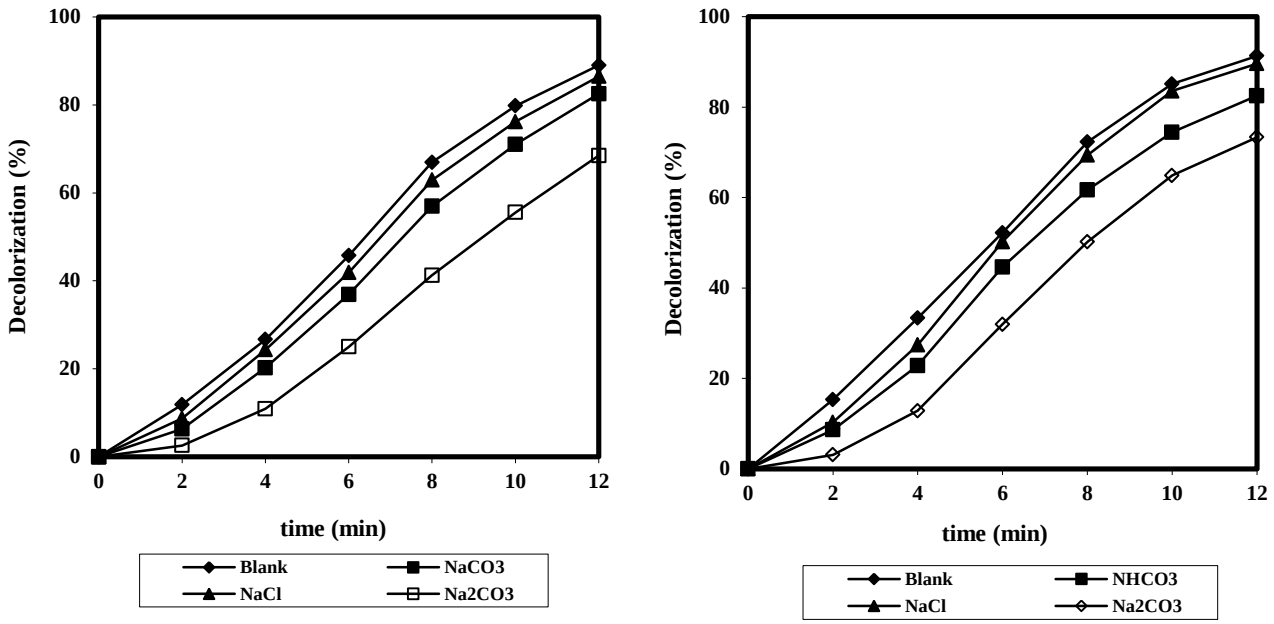

Figure 7: The effect of inorganic anions on the decolorization of dyes using photocatalytic ozonation (a) RRRB and (b) DGB (0.02 M of salts, Ozone concentration: 55 g/m^3, 5 mg/L of NFN and 1 L of dye solution (150 mg/L) at room temperature (25 °C)).

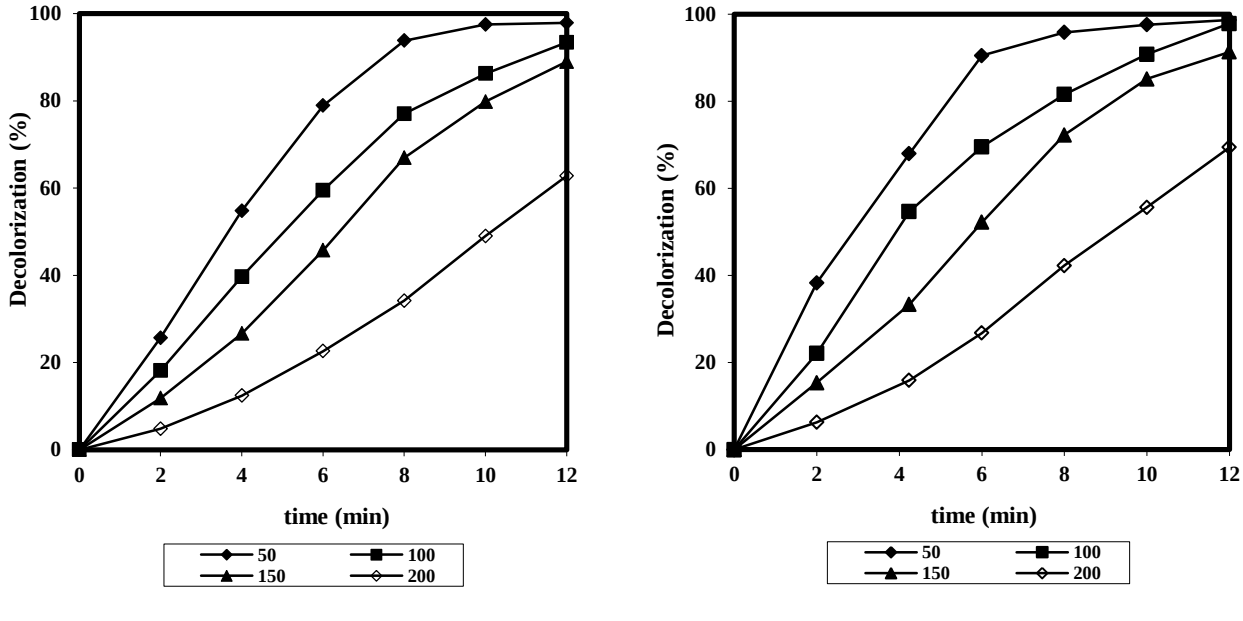

Figure 8: The effect of dye concentration (mg/L) on the decolorization of dyes using photocatalytic ozonation (a) RRRB and (b) DGB (5 mg/L of NFN, Ozone concentration: 55 g/m^3, and 1 L of dye solution at pH=3).

4. Conclusion

Photocatalytic ozonation of dyes using Nickel ferrite nanoparticle (NFN) was investigated. The reaction parameters studies showed that dyes were decolorized and degraded using NFN nanoparticle. Aliphatic carboxylic acids were detected as dominant aliphatic intermediates where, they were further oxidized slowly to CO_2. Inorganic anions were detected as the products of photocatalytic ozonation mineralization of dyes. Results showed that the NFN nanocatalyst is effective to degrade textile dye. This technique may be viable for treatment of large volumes of aqueous colored dye solutions. Photocatalytic ozonation using NFN nanocatalyst is capable of decolorizing and treating colored textile wastewaters without using high oxygen pressure or heating.

5. References

1. M. E. Olya, M. Madadi, F. Tadayon, Synthesis, characterization and application of nano-composite silica aerogel- egg shell for dye removal of colored wastewater. *Prog. Color Colorant. Coat.*, 9(2016), 1-16.
2. A. A. El-Zahhar, N. S. Awwad, Removal of malachite green dye from aqueous solutions using organically modified hydroxyapatite. J. *Environ. Chem. Eng.*, 4(2016), 633-638.
3. J. Si, B. K. Cui, Y. Yuan,Y. C. Dai, Biosorption performances of raw and chemically modified biomasses from Perenniporiasubacida for heterocycle dye Neutral Red. *Desalin. Water Treat.*, 57(2016), 8454-8469.
4. S. S. Batool, Z. Imran, S. Hassan, K. Rasool, M. Ahmad, M. A. Rafiq, Enhanced adsorptive removal of toxic dyes using SiO_2 nanofibers. *Solid State Sci.*, 55(2016), 13-20
5. J. Shi, T. Wu, K. Teng, W. Wang, M. Shan, Z. Xu, H. Lv, H. Deng. Simultaneous electrospinning and spraying toward branch-like nanofibrous membranes functionalised with carboxylated MWCNTs for dye removal. *Mater. Lett.*, 166(2016), 26-29.
6. I. Altın, M. Sökmen, Z. Bıyıklıoğlu, Sol gel synthesis of cobalt doped TiO_2 and its dye sensitization for efficient pollutant removal. *Mater. Sci. Semicond. Process.*, 45(2016), 36-44.
7. F. Han, H. Li, J. Yang, X. Cai, L. Fu. One-pot synthesis of cuprous oxide-reduced graphene oxide nanocomposite with enhanced photocatalytic and electrocatalytic performance. *Physica E*, 77(2016),122-126.
8. Y. Zheng, L. Fu, F. Han, A. Wang, W. Cai, J. Yu, J. Yang, F. Peng. Green biosynthesis and characterization of zinc oxide nanoparticles using Corymbiacitriodora leaf extract and their photocatalytic activity. *Green Chem. Let. Rev.*, 8(2015), 59-63.
9. L. Fu, T. Xia, Y. Zheng, J. Yang, A. Wang, Z. Wang. Preparation of WO_3-reduced graphene oxide nanocomposites with enhanced photocatalytic property. *Ceramics Int.*, 41(2015), 5903-5908
10. J. Nawrocki, B. Kasprzyk-Hordern. The efficiency and mechanisms of catalytic ozonation. *Appl. Catal. B: Environ.*, 99(2010), 27.
11. T. E. Agustina, H. M. Ang, V. K. Vareek, A review of synergistic effect of photocatalysis and ozonation on wastewater treatment. *J. Photochem. Photobiol. C: Photochem. Rev.*, 6(2005),264.
12. B. K. Hordern, M. Ziolek, J. Nawrocki, Catalytic ozonation and methods of enhancing molecular ozone reactions in water treatment, *Appl. Catal. B: Environ.*, 46(2003), 639.
13. M. Mehrjouei, S. Muller, D. Moller, Degradation of oxalic acid in a photocatalyticozonation system by means of Pilkington Active glass, *J. Photochem. Photobiol. A: Chem.*, 217(2011), 417.
14. Y. Jing, L. Li, Q. Zhang, P. Lu, P. Liu, X. Lü, Photocatalyticozonation of dimethylphthalate with TiO_2 prepared by a hydrothermal method, *J. Hazard. Mater.*, 189(2011), 40-47.
15. F. J. Beltran, A. Aguinaco, J. F. García-Araya, Kinetic modelling of TOC removal in the photocatalyticozonation of diclofenac aqueous solutions, *Appl. Catal. B: Environ.*, 100(2010), 289.
16. S. Nishimoto, T. Mano, Y. Kameshima, M. Miyake, Photocatalytic water treatment over WO_3 under visible light irradiation combined with ozonation, *Chem. Phys. Lett.*, 500(2010), 86.
17. T. Oyama, I. Yanagisawa, M. Takeuchi, T. Koike. Remediation of simulated aquatic sites contaminated with recalcitrant substrates by

TiO_2/ozonation under natural sunlight, *Appl. Catal. B. Environ.*, 1(2009), 242.
18. R. Rajeswari, S. Kanmani, A study on synergistic effect of photocatalyticozonation for carbaryl degradation, *Desalination.*, 242(2009), 277.
19. L. Zou, B. Zhu, The synergistic effect of ozonation and photocatalysis on color removal from reused water, *J. Photochem. Photobiol. A. Chem.*, 196(2008), 24.
20. F. J. Beltran, A. Aguinaco, J. F. Garcıa-Araya, A. Oropesa, Ozone and photocatalytic processes to remove the antibiotic sulfamethoxazole from water, *Water Res.*, 42(2008), 3799.
21. M. J. Farre, M. I. Franch, J. A. Ayllón, J.Peral, X. Domenech, Biodegradability of treated aqueous solutions of biorecalcitrant pesticides by means of photocatalyticozonation, *Desalination.*, 211(2007), 22.
22. A. M. Amat, A. Arques, M. A. Miranda, S. Segui, R. F. Vercher, Degradation of rosolic acid by advanced oxidation processes: ozonation vs. solar photocatalysis, *Desalination*, 212(2007), 114.
23. J. S. Hur, S. O. Oh, K. M. Lim, J. S. Jung, J. W. Kim, Y. J. Koh, Novel effects of TiO_2 photocatalytic ozonation on control of postharvest fungal spoilage of kiwifruit, *Postharvest Biol. Technol.*, 35(2005), 109.
24. L. Li, W. Zhu, L. Chen, P. Zhang, Z. Chen, Photocatalyticozonation of dibutyl phthalate over TiO2 film. *J. Photochem. Photobiol. A. Chem.*, 175(2005), 172.
25. M. Addamo, V. Augugliaro, E. G. Lopez, V. Loddo, G. Marci, L. Palmisano, Oxidation of oxalate ion in aqueous suspensions of TiO_2 by photocatalysis and ozonation, *Catal. Today.*, 107-108(2005), 612.
26. D. L. Pavia, G. M. Lampman, G. S. Kaiz, Introduction to Spectroscopy: A Guide for Students of Organic Chemistry, W. B. Saunders Company, 1987.
27. J. Wang, F. Ren, B. Jia, X. Liu, Solvothermal synthesis and characterization of $NiFe_2O_4$ nanospheres with adjustable sizes. *Solid State Comm.*, 150(2010), 1141.
28. K. Tanaka, S. M. Robledo, T. Hisanaga, R. Ali, Z. Ramli, W. A. Bakar, Photocatalytic degradation of 3,4-xylyl N-methylcarbamate (MPMC) and other carbamate pesticides in aqueous TiO_2 suspensions. *J. Mol. Catal. A: Chem.*, 144(1999), 425.
29. I. K. Konstantinou, T. A. Albanis, TiO_2-assisted photocatalytic degradation of azo dyes in aqueous solution: kinetic and mechanistic investigations-a review, *Appl. Catal. B: Environ*,. 49(2004), 1.
30. O. Gimeno, M. Carbajo, M. J. Lopez, J. A. Melero, F. J. Beltran, F. J. Rivas. Photocatalytic promoted oxidation of phenolic mixtures: an insight into operating and mechanistic aspects. *Water Res.*, 41(2007), 4672.
31. I. Arsalan-Alaton, A review of the effects of dye-assisting chemicals on advanced oxidation of reactive dyes in wastewater, *Color. Technol.*, 119(2003), 345.

How to cite this article:
N. M. Mahmoodi, Photocatalytic Degradation of Textile Dyes Using Ozonation and Magnetic Nickel Ferrite Nanoparticle, Prog. Color Colorants Coat., 9 (2016) 163-171.